blood

2012 120: 2757-2767
Prepublished online August 16, 2012;
doi:10.1182/blood-2012-05-429936

The interplay between the Rab27A effectors Slp4-a and MyRIP controls hormone-evoked Weibel-Palade body exocytosis

Ruben Bierings, Nicola Hellen, Nikolai Kiskin, Laura Knipe, Ana-Violeta Fonseca, Bijal Patel, Athina Meli, Marlene Rose, Matthew J. Hannah and Tom Carter

Blood (print ISSN 0006-4971, online ISSN 1528-0020), is published weekly by the American Society of Hematology, 2021 L St, NW, Suite 900, Washington DC 20036.

The interplay between the Rab27A effectors Slp4-a and MyRIP controls hormone-evoked Weibel-Palade body exocytosis

*Ruben Bierings,[1] *Nicola Hellen,[1] Nikolai Kiskin,[1] Laura Knipe,[1] Ana-Violeta Fonseca,[1] Bijal Patel,[1] Athina Meli,[2] Marlene Rose,[2] Matthew J. Hannah,[1] and Tom Carter[1]

[1]Medical Research Council National Institute for Medical Research, The Ridgeway, London, United Kingdom; and [2]Faculty of Medicine, Imperial College London, London, United Kingdom

Weibel-Palade body (WPB) exocytosis underlies hormone-evoked VWF secretion from endothelial cells (ECs). We identify new endogenous components of the WPB: Rab3B, Rab3D, and the Rab27A/Rab3 effector Slp4-a (granuphilin), and determine their role in WPB exocytosis. We show that Rab3B, Rab3D, and Rab27A contribute to Slp4-a localization to WPBs. siRNA knockdown of Slp4-a, MyRIP, Rab3B, Rab3D, Rab27A, or Rab3B/Rab27A, or overexpression of EGFP-Slp4-a or EGFP-MyRIP showed that Slp4-a is a positive and MyRIP a negative regulator of WPB exocytosis and that Rab27A alone mediates these effects. We found that ECs maintain a constant amount of cellular Rab27A irrespective of the WPB pool size and that Rab27A (and Rab3s) cycle between WPBs and a cytosolic pool. The dynamic redistribution of Rab proteins markedly decreased the Rab27A concentration on individual WPBs with increasing WPB number per cell. Despite this, the probability of WPB release was independent of WPB pool size showing that WPB exocytosis is not determined simply by the absolute amount of Rab27A and its effectors on WPBs. Instead, we propose that the probability of release is determined by the fractional occupancy of WPB-Rab27A by Slp4-a and MyRIP, with the balance favoring exocytosis. (*Blood*. 2012;120(13):2757-2767)

Introduction

Hormone-evoked VWF secretion from endothelial cells (ECs) is mediated by exocytosis of specialized secretory granules (SGs) called Weibel-Palade bodies (WPBs).[1] WPB exocytosis is triggered by increases in intracellular free Ca^{2+} or cAMP concentrations, and involves a number of molecular components, including the N-ethylmaleimide–sensitive factor, VAMP3, SNAP23, syntaxin 4, RalA, the annexin A2/S100A10 complex, and phospholipase D.[2-7]

In addition, Rab proteins also regulate WPB exocytosis. A subset of Rab proteins, including Rab3A-3D, Rab27A/B, and Rab37, is associated with SGs in different cell types where they regulate SG biogenesis, trafficking, and exocytosis.[8] Secretory cells often express a mixture of these "secretory" Rabs, which may have overlapping or distinct functions. Human ECs are reported to express mRNA for Rab3A, Rab3D, and Rab37,[3,9,10] Rab3B protein,[11] and Rab27A mRNA and protein.[12,13] To date, Rab27A is the only endogenous EC Rab protein that has been detected on WPBs. Through its effector MyRIP and Myosin Va, Rab27A is proposed to negatively regulate WPB exocytosis.[13,14] Rab27A can interact with different effector molecules, and many secretory cells express a mixture of these effectors.[8] In these cases, SG exocytosis probably depends on the balance of Rab27A interactions with the complement of Rab effectors in the cell.

In addition to MyRIP, ECs contain mRNA for the Rab27A effector Slp4-a (granuphilin).[13] Slp4-a links SGs to the plasma membrane (PM) through SG-associated Rab proteins (principally Rab27A), PM-associated syntaxins (1a, 2, or 3) and soluble Munc18 isoforms.[15-19] Syntaxins exist in open and closed conformations that determine their participation in SNARE complex formation and membrane fusion. Slp4-a binds the closed conformation of syntaxin,[16,19] which selectively interacts with Munc18 proteins to hold SGs in a fusion-incompetent state at the PM. Overexpression of Slp4-a increased numbers of PM-docked SGs but inhibited secretion, whereas knockout or knockdown (KD) studies showed the opposite.[20] Unlike MyRIP, Slp4-a interacts with several different Rab proteins, including Rab3A-3D and Rab8,[15,21] and with myosin Va,[22] a point of convergence with MyRIP.

In this study, we identified Slp4-a, Rab3B, and Rab3D as new components of WPBs and investigated their roles in regulating hormone-evoked WPB exocytosis and VWF secretion. We found that, in contrast to other secretory cells, Slp4-a acts as a positive regulator of WPB exocytosis, and its interplay with the negative regulator MyRIP on Rab27A bound to WPBs (WPB-Rab27A) sets the probability of WPB exocytosis.

Methods

Tissue culture, transfection, secretion assays, antibodies, DNA constructs, and reagents

Primary HUVECs were purchased, cultured and transfected as previously described.[23] Human aortic endothelial cells (HAECs) were cultured as previously described.[24] Secreted VWF and EGFP were assayed by ELISA as previously described.[25] Primary antibodies (Abs) along with the dilutions for immunofluorescence and Western blotting are given in supplemental Table 1A (available on the *Blood* Web site; see the Supplemental Materials

Submitted May 14, 2012; accepted July 31, 2012. Prepublished online as *Blood* First Edition paper, August 16, 2012; DOI 10.1182/blood-2012-05-429936.

*R.B. and N.H. contributed equally to this study.

The online version of this article contains a data supplement.

The publication costs of this article were defrayed in part by page charge payment. Therefore, and solely to indicate this fact, this article is hereby marked "advertisement" in accordance with 18 USC section 1734.

link at the top of the online article) with sources of secondary Abs appended. Production of an anti-Rab27A Ab is described in supplemental Figure 1A. DNA constructs are described in the supplemental Appendix 1. Primers for amplification of full-length Rab3 isoforms, MyRIP and Slp4-a, are listed in supplemental Table 1B. All reagents were from Sigma-Aldrich unless otherwise stated. Fura-2/AM was from Invitrogen.

Immunoblotting

Cells were rinsed with PBS and lysed in 2× sample buffer[12] containing β-mercaptoethanol and protease inhibitors (Sigma-Aldrich: P8340) or in PBS containing 1% Triton X-114, 2mM EDTA, and protease inhibitors. To concentrate hydrophobic proteins, Triton X-114 partitioning of the lysate was performed as described.[12] Protein in the detergent phase was precipitated with methanol-chloroform using 0.25 μg BSA as carrier. Proteins were separated on a 12% SDS-PAGE gel, transferred to 0.2 μm nitrocellulose membrane, and probed with primary Ab, followed by infrared dye-coupled secondaries. Membranes were scanned with the LI-COR Odyssey Infrared Imaging system (LI-COR Biosciences).

RNAi

Pools of 4 siRNA oligo duplexes (ON-TARGET*plus* SMARTpool, Dharmacon RNA Technologies) were used to deplete HUVECs of the mRNAs of Rab27A (#L004667), Rab3B (#L008825), Rab3D (#L010822), Slp4-a (#L007111), and MyRIP (#L013964). Oligo sequences are in supplemental Table 1C. A pool of 4 nontargeting siRNAs (ON-TARGET*plus* Nontargeting pool, #D001810) was used as a control (siCTRL). A total of 1000 pmol of siRNA duplexes was transfected by nucleofection into 7.5×10^6 HUVECs. ECs were plated at confluent density ($\sim 0.8 \times 10^5$ cells/cm^2) in gelatin-coated wells of 6- or 12-well plates or on gelatin-coated glass coverslips and cultured in HUVEC growth medium for 48 hours. Depletion of Rab27A, Rab3B, Rab3D, Slp4-a, and MyRIP was assessed by quantitative PCR, immunocytochemistry, or immunoblotting.

RT-PCR and quantitative PCR analysis

RNA was extracted using RNeasy Mini Kit (QIAGEN) and integrity verified on a 2100 Bioanalyzer (Agilent Technologies). cDNA was synthesized using a QuantiTect Reverse Transcription kit (QIAGEN) from 500 ng of RNA. RT-PCR primers for Rab3A to Rab3D are in supplemental Table 1D. The cycling protocol was: initial 95°C for 30 seconds followed by 30 cycles of 95°C for 15 seconds, 52°C for 30 seconds, 68°C for 15 seconds, final 5 minutes at 72°C and products run on 2% agarose gel. Alternative primers and cycling conditions for Rab3A were also used.[9] Quantitative PCR primers for reference genes (RGs: ACTB, GAPDH, B2M, UBC, YWHAZ, SF3A1, CYC1, EIF4A2, SDHA [housekeeping gene detection kit]), Rab27A, Slp4-a, MyRIP, Rab3B, and Rab3D were designed and synthesized by PrimerDesign LTD (supplemental Table 1D). Amplification was detected using Sensimix (Bioline) and analyzed on a Rotor-gene 6000 (Corbett Life Science) using 95°C for 10 minutes, then 40-45 cycles of 10 seconds at 95°C, 15 seconds at 60°C, and 20 seconds at 72°C, followed by a 5-minute melt sequence to verify single amplicons. Single products were further verified on 2% agarose gels and extracted (GenElute gel extraction kit) for standard curve generation. Absolute copy number was determined and normalized to β-actin (ACTB) expression. For KD experiments, cDNA samples were first screened for RG expression levels, and geNorm Version 3.4 software (PrimerDesign LTD) was used to determine normalization factors before normalization. Quantification was calculated using the ΔΔCT method.[26]

Immunocytochemistry and quantification of antigen immunoreactivity on WPBs

Immunostaining and imaging of fixed cells were performed as previously described.[25] For both confocal (40× objective) and wide-field (100× objective) intensity measurements, exposures at each wavelength were first set to ensure no detector saturation on the brightest sample and then kept constant for all images. Images were processed in ImageJ (http://rsbweb.nih.gov/ij/) and numbers of WPBs quantified as previously described.[25] Mean WPB fluorescence intensities (FIs) for endogenous Rab27A, MyRIP, Slp4-a, Rab3B immunoreactivity (IR) or for EGFP-Rab27A, -MyRIP or -Slp4-a were determined from background-subtracted regions of interest (ROI) enclosing individual WPBs. Two (Slp4-a, MyRIP) or 3 (Rab27A) independent experiments were performed using 6-12 (confocal) or > 50 (wide-field) fields of view in which > 12 WPBs/per cell were analyzed in cells from a minimum of 10 (confocal) or 1 or 2 (wide-field) cells.

Live cell imaging

Exocytosis of Proregion-EGFP-containing WPBs was determined as previously described.[23,25] The moment of WPB fusion for EGFP-Rab27A– or EGFP-Slp4-a–expressing cells was determined by an abrupt decrease in WPB fluorescence on fusion (illustrated for Rab27A in supplemental Figure 1B). The probability of WPB exocytosis, P_r, was determined as the mean percentage of degranulation of fluorescent WPBs after cell stimulation. The mean WPB-EGFP FI for EGFP-Rab27A was determined as described in "Immunocytochemistry and quantification of antigen immunoreactivity on WPBs." Rab acquisition by immature WPBs was determined by time-lapse imaging of ECs expressing VWF-tdTomato (VWF-tdT) and EGFP-Rab27A or mEGFP-Rab3B (16 hours after nucleofection). Microscope and experimental details are in the legend to supplemental Video 1. Mean WPB-EGFP and WPB-tdT FIs were determined from background-subtracted images as described in the previous section.

Whole-WPB fluorescence recovery analysis of Rabs and effectors cycling on WPBs

Leica TCS SP2 or Leica TCS SP5 confocal microscopes equipped with PL APO 100 × 0.7-1.4NA (SP2) or HCX PL APO CS 100 × 1.46NA (SP5) objectives were used to study fluorescence recovery after whole WPB bleaching (FRAP) at 37°C. Imaging and bleaching settings were as previously described.[27] For FRAP, 1-2 pulses at full laser power were applied to a bleaching ROI encompassing the entire WPB, and the WPB FI followed to monitor recovery. For whole-cell inverse FRAP (iFRAP[28]) a PL APO 63 × 0.6-1.4NA objective was used to image at least 2 fluorescent cells at a time. All but a small region of 1 cell (containing a few WPBs) was bleached using full laser power pulses at 1- to 2-second intervals over an ~ 5-minute period. The decline in FI in the unbleached region of the test cell was followed at 1- to 10-minute intervals. For analysis, ROIs were defined by thresholding low-pass filtered images above the background to include just the bleached WPB (FRAP) or unbleached (iFRAP) WPBs in the cell. The average FI within the ROIs was scaled by the decline because of bleaching in adjacent unbleached control cells/WPBs in the image. Exponential fitting was performed in Origin Version 8.5 (OriginLab) without constraints on offset or final level.

Statistical analysis

Data were plotted in Origin Version 7.5 or greater or GraphPad Prism Version 5.0. Statistical analysis was by nonparametric *t* test (except where indicated) using GraphPad Prism Version 5.0. Significance values are shown on the figures or in figure legends. Data are shown as mean ± SEM.

Results

Slp4-a is localized to WPBs

Identification of Slp4-a mRNA in HUVECs[13] led us to examine whether this Rab27A effector was associated with WPBs and played a role in regulating WPB exocytosis. Endogenous Slp4-a-IR was readily detectable on WPBs in HUVECs (Figure 1A; supplemental Figure 2A) and adult HAECs (supplemental Figure 2B). Furthermore, expression of EGFP-Slp4-a specifically labeled WPBs (eg, see Figure 4Ci). However, several observations indicate that Rab27A is not solely responsible for recruiting Slp4-a to WPBs. First, HUVECs with few WPBs (eg, * in Figure 1B) consistently

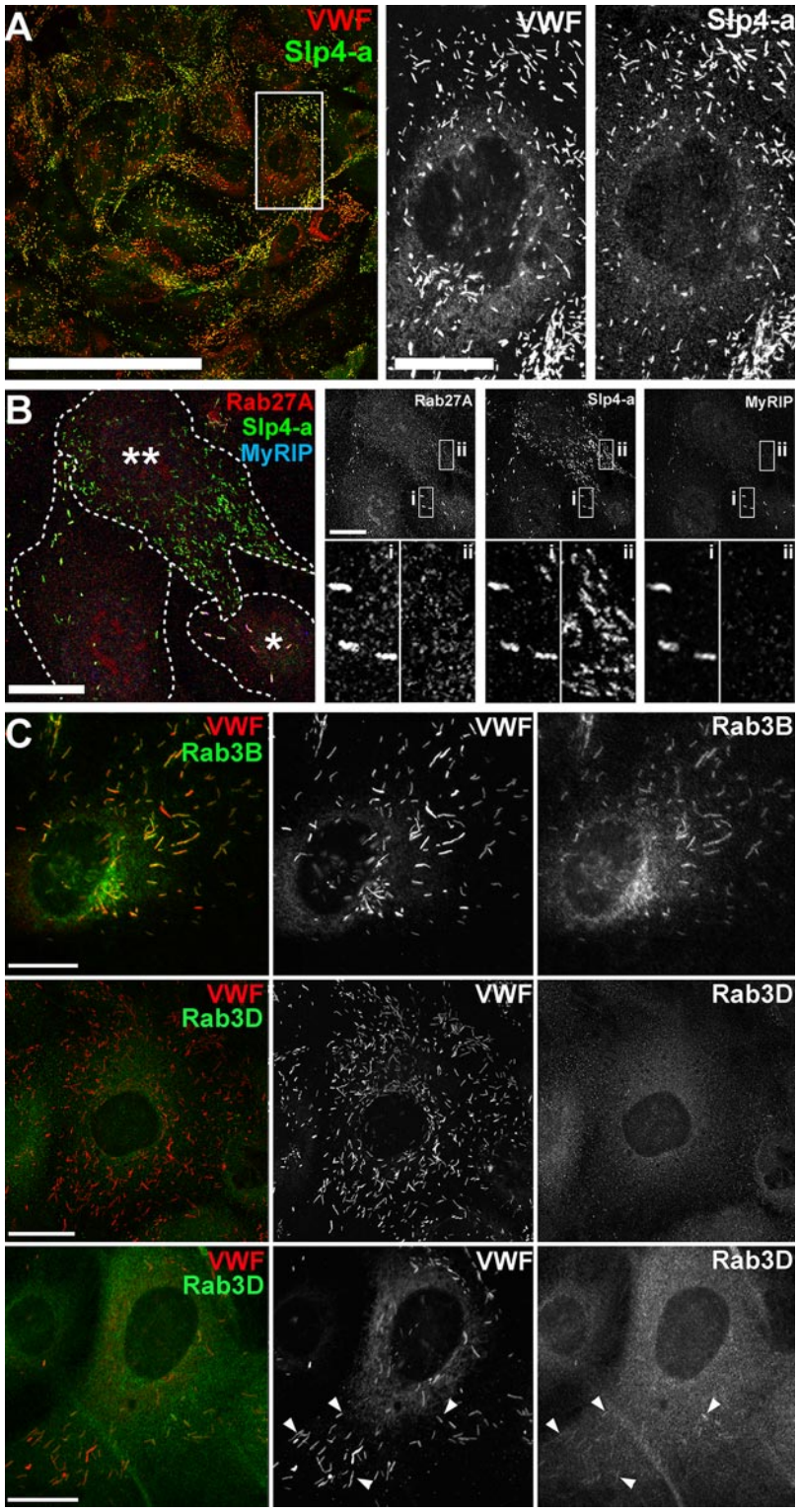

Figure 1. Endogenous Slp4-a, Rab3B, and Rab3D are expressed in HUVECs and localize to WPBs. (A) HUVECs immunolabeled for endogenous VWF (red) and Slp4-a (green). The intensity levels of the red (VWF) channel were adjusted from 0-255 to 0-130 intensity units. Scale bar represents 200 μm. Grayscale images are from the region indicated by the white box (scale bar represents 20 μm). (B) Left: HUVECs immunolabeled for endogenous Rab27A (red), Slp4-a (green), and MyRIP (blue). Scale bar represents 20 μm. Dashed white lines indicate approximate cell boundaries and a cell with few (*) and a cell with many (**) WPBs are indicated. Right top: Grayscale images are shown for each channel as indicated and the subregions i and ii shown on expanded scales below. (C) HUVECs immunolabeled for endogenous Rab3B (mouse Ab, green) or Rab3D (mouse Ab, green) and VWF (rabbit Ab, red). Top: Endogenous Rab3B-IR is localized to WPBs. Middle: > 95% of cells had no WPB-Rab3D-IR (see also supplemental Figure 4Civ). Bottom: < 5% of cells had weak WPB-Rab3D-IR (arrowheads). Scale bars represent 10 μm. Immunofluorescence images of fixed cells here and in all subsequent figures were taken at room temperature using Leica SP1 or SP2 confocal microscopes and software (Version 2.61, build 1537) equipped with 40× and 100× objectives (SP1; PL APO40 × 1.25-0.75NA, PL APO100 × 1.4NA, SP2; HCX PL APO40 × 1.2 NA, PL APO100 × 1.4NA).

had strong WPB-Rab27A-IR, whereas HUVECs with large numbers of WPBs (**) had almost undetectable WPB-Rab27A-IR (see also supplemental Figure 3A-B; quantified in Figure 6A). Control experiments showed the intensity of WPB-Rab27A-IR was proportional to WPB-Rab27A-antigen concentration (supplemental Figure 3C), so the reduction in WPB-Rab27A-IR reflects a reduction in WPB-Rab27A concentration. This pattern was mirrored by endogenous WPB-MyRIP-IR but not by WPB-Slp4-a-IR, which remained prominent irrespective of WPB number, and the same was seen in HAECs (Figure 1B; supplemental Figures 2 and 3B,D). Second, KD of Rab27A in HUVECs resulted in loss of both WPB-Rab27A- and WPB-MyRIP-IR, but not of WPB-Slp4-a-IR (supplemental Figure 3E). Finally, we observed a subpopulation of Rab27A-negative WPBs displaying Slp4-a-IR (Figure 2D). Because Slp4-a can also bind Rab8 and Rab3A-3D[15,21] (and supplemental Figure 4A), we next looked for the expression and WPB localization of these Rab proteins. Although HUVECs express Rab8,[11,29] we detected neither endogenous nor epitope-tagged Rab8

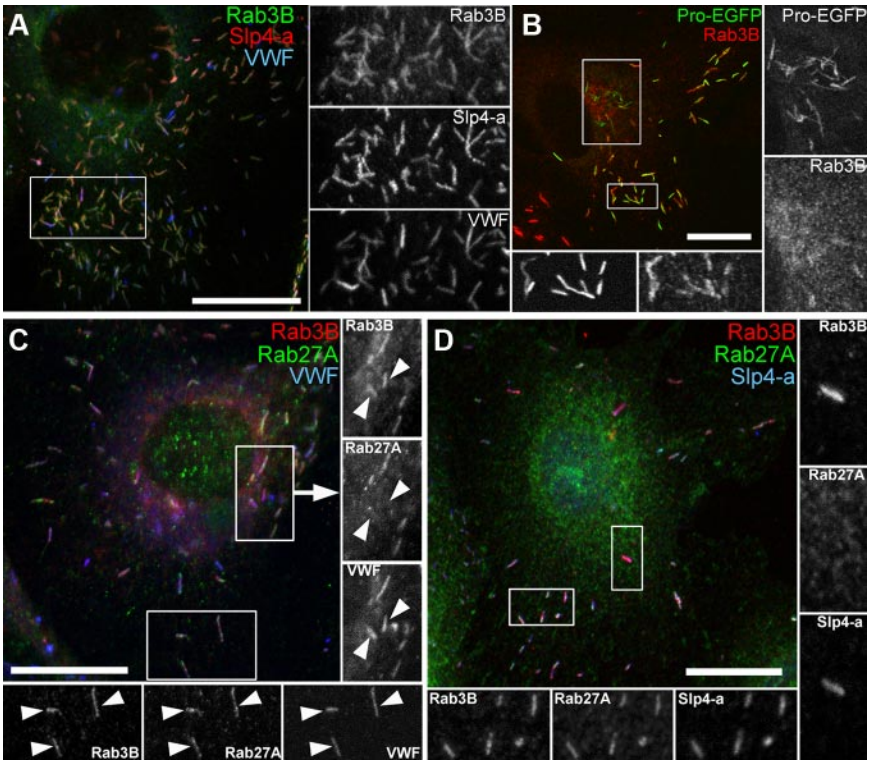

Figure 2. Rab3B is detectable on WPBs before Rab27A and colocalizes with Slp4-a. (A) HUVECs immunolabeled for endogenous Rab3B (mouse Ab, green), Slp4-a (rabbit Ab, red), and VWF (sheep Ab, blue). Here and in other figures, grayscale images are from regions indicated by white boxes. (B) HUVECs expressing Proregion-EGFP (Pro-EGFP, green, 24 hours after nucleofection) immunolabeled for endogenous Rab3B (mouse Ab, red). Grayscale images represent regions with perinuclear immature (right) or peripheral mature WPBs (bottom). (C) HUVECs immunolabeled for Rab3B (mouse Ab, red), Rab27A (rabbit Ab, green), and VWF (sheep Ab, blue). Insets: right, arrowheads point to Rab3B-positive, Rab27A-negative perinuclear immature WPBs; bottom, Rab3B- and Rab27A-positive mature WPBs. (D) HUVECs immunolabeled for Rab3B (goat Ab; red), Rab27A (mouse Ab, green), and Slp4-a (rabbit Ab, blue). Inset: right, Rab3B-positive, Rab27A-negative, Slp4-a-positve perinuclear immature WPBs; bottom, mature WPBs positive for all markers. Scale bars represent 10 μm.

on WPBs. We therefore focused on Rab3 isoforms (specificities of the Rab3 reagents are shown in supplemental Figure 4Bi-vi).

Rab3B and Rab3D are expressed in ECs and localized to WPBs

Expression of mEGFP-Rab3A-3D labeled WPBs in HUVECs (supplemental Figure 4Bii-vi); however, immunostaining showed that only endogenous Rab3B-IR was clearly detectable on WPBs in HUVECs (and HAECs), whereas WPB-Rab3D-IR was weakly detectable in only ~ 5% of cells (Figure 1C; supplemental Figure 4C-D). RT-PCR and Western blot analysis confirmed that only Rab3B and Rab3D were expressed in HUVECs (supplemental Figure 4E). No Rab3A mRNA was found despite using primers and conditions reported to detect this Rab in HUVECs[9] (supplemental Figure 4E). Quantitative PCR quantification showed that Rab3B and Rab3D transcripts together were > 10 times more abundant than Rab27A transcripts.

Unlike WPB-Rab27A-IR, WPB-Rab3B-IR was clearly observed irrespective of WPB pool size and matched closely the pattern for endogenous Slp4-a-IR (Figure 2A). Similar to Rab27A,[12] Rab3B-IR was absent from most newly formed WPBs at the trans-Golgi network (Figure 2B); however, we observed a subpopulation of immature Rab27A-negative WPBs that were Rab3B-positive (Figure 2C) and displayed clear Slp4-a-IR (Figure 2D). Together, the data show that Rab27A is not the sole Slp4-a-interacting Rab protein on WPBs and that the WPB localization of Rab3B matches closely that of Slp4-a.

Rab3B is recruited slowly to immature WPBs but cycles rapidly on mature WPBs where it recruits Slp4-a

Because differences in the kinetics of recruitment of Rab3B and Rab27A to immature WPBs might account for Rab3B-IR on perinuclear Rab27A-negative WPBs, we next determined the time constants of recruitment (τ_{recr}) of mEGFP-Rab3B and EGFP-Rab27A to immature VWF-tdT–expressing WPBs in live cells (eg, supplemental Video 1). τ_{recr} for mEGFP-Rab3B and EGFP-Rab27A were not significantly different (Figure 3A), indicating that other factors may account for this phenomenon (see "Discussion").

To investigate whether Rab3B or Rab3D might contribute to WPB recruitment of Slp4-a, we performed WPB bleaching experiments. The rationale for FRAP experiments was that Rab proteins and their effectors exchange (cycle) between their target membranes and the cytosol, and that this process, for both Rabs and effectors, is linked to the Rab GTP-GDP cycle.[30] Where an effector (Slp4-a) has access to a mixture of different Rabs, as is potentially the case here, the cycling kinetics will reflect a composite function of the kinetics of the individual Rabs of the mixture. Thus, by determining the association time constants (τ_{ass}) for individual WPB-Rabs and comparing τ_{ass} for Slp4-a cycling on WPBs expressing exogenous Rab27A, Rab3B, or Rab3D with Slp4-a cycling in the absence of expressed WPB-Rabs, we might identify with which WPB-Rab Slp4-a interacts.

We quantified τ_{ass} for EGFP-tagged Rab27A, Rab3B, or Rab3D after whole WPB bleaching. EGFP-Rab27A recovered very slowly and often incompletely during the observation period (Figure 3B). mRFP-Rab27A behaved like EGFP-Rab27A. mEGFP-Rab3B and -Rab3D recovered significantly faster than EGFP-Rab27A (Figure 3B,D). Dissociation time constants (τ_{diss}) for EGFP-Rabs, determined by iFRAP, were of similar magnitude to τ_{ass} (Figure 3B-C), both probably reflecting the off-rates of Rab unbinding from the WPB.[31] For mEGFP-Rab3B, both τ_{ass} and τ_{diss} were significantly faster than for EGFP-Rab27A.

τ_{ass} for EGFP-Slp4a to WPBs coexpressing exogenous mRFP-tagged Rab27A, Rab3B, or Rab3D were, in each case, similar to those of the Rab protein alone (Figure 3D-E). Notably, EGFP-Slp4-a when expressed alone recovered fast, with a τ_{ass} similar to that seen in the presence of exogenous Rab3B (or Rab3D; Figure

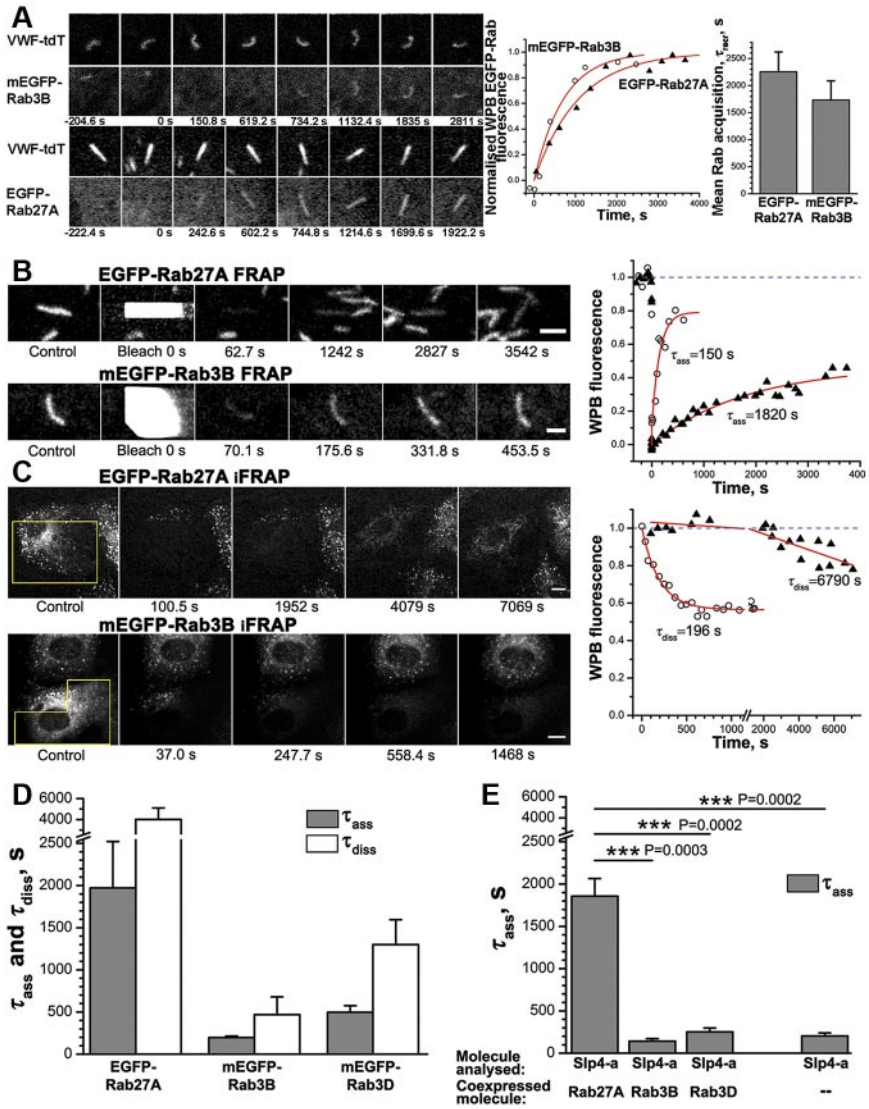

Figure 3. Rab recruitment to and cycling on WPBs: evidence for association of EGFP-Slp4-a with Rab3s on mature WPBs. (A) Left: Images from time-lapse videos showing Rab acquisition by immature VWF-tdT containing WPBs in HUVECs coexpressing either mEGFP-Rab3B (top) or EGFP-Rab27A (bottom). Times are indicated below the panels. Right: Example time courses of mEGFP-Rab3B (○, τ_{recr} 709 seconds) or EGFP-Rab27A (▲, τ_{recr} 1070 seconds) recruitment to VWF-tdT–labeled WPBs. Bar plot represents the mean values of τ_{recr} for WPB-mEGFP-Rab3B (1730 ± 355 seconds, n = 7) and WPB-EGFP-Rab27A (2260 ± 365 seconds, n = 9) were not significantly different (P = .35). (B) Left: Images from FRAP experiments with WPB-EGFP-Rab27A (top; scale bar represents 2 μm) and WPB-mEGFP-Rab3B (bottom; scale bar represents 1 μm) show FI recovery after complete WPB bleaching (FRAP, t = 0 seconds). Times are indicated below frames. Right: Average WPB mEGFP-Rab3B (○) and EGFP-Rab27A (▲) FIs normalized to the prebleach levels. Graphs were fitted with exponential association functions $A \times [1 - \exp(-t/\tau_{ass})]$. Unconstrained fits to fluorescence recovery reached 0.80 for Rab3B and 0.63 for Rab27A. (C) Left: Images from iFRAP experiments with EGFP-Rab27A (top) and mEGFP-Rab3B (bottom). Scale bars represent 10 μm. Regions indicated by boxes were continuously bleached for 5 minutes, then FI of unbleached WPBs was measured. Fluorescence of neighboring cells was used for control. Times after bleaching are indicated below frames. Right: Average FIs of WPB-mEGFP-Rab3B (○) and WPB-EGFP-Rab27A (▲) were normalized to the initial postbleach levels. Graphs were fitted with exponential decay functions $A \times \exp(-t/\tau_{diss})$. (D) Average cycling time constants determined for each EGFP-Rab by FRAP (τ_{ass}, gray) and iFRAP (τ_{diss}, white) were as follows: EGFP-Rab27A, 1970 ± 550 seconds (n = 8) and 4020 ± 1090 seconds (n = 6); mEGFP-Rab3B, 196 ± 18 seconds (n = 6) and 468 ± 211 seconds (n = 5); mEGFP-Rab3D, 496 ± 79 seconds (n = 8) and 1300 ± 296 seconds (n = 8), respectively. The τ_{ass} (FRAP) for mEGFP-Rab3B and Rab3D were significantly faster than for EGFP-Rab27A (P = .0007 and P = .002, respectively). The τ_{diss} (iFRAP) for mEGFP-Rab3B was also significantly faster than for EGFP-Rab27A (P = .017). (E) Average τ_{ass} for EGFP-Slp4-a coexpressed with RFP-tagged Rab27A (n = 8), Rab3B (n = 7), Rab3D (n = 8), or alone (n = 14) as indicated. τ_{ass} for EGFP-Slp4-a coexpressed with Rab3B or Rab3D were not different from that for EGFP-Slp4-a alone (P = .31 and P = .43, respectively), whereas they were significantly faster than τ_{ass} with mRFP-Rab27A coexpression.

3E). This indicates that Slp4-a can interact with endogenous Rab3B and/or Rab3D on WPBs.

Analysis of Slp4-a, MyRIP, and WPB-Rab function in WPB exocytosis

Slp4-a is a positive and MyRIP a negative regulator of WPB exocytosis. To assess the function of Slp4-a in hormone-evoked WPB exocytosis, we depleted endogenous Slp4-a by siRNA KD and for comparison analyzed the effect of MyRIP KD. Slp4-a KD (Figure 4A) substantially decreased while MyRIP KD (Figure 4B) increased histamine-evoked VWF secretion. To examine the effect of overexpression of EGFP-Slp4-a or EGFP-MyRIP on Ca^{2+}-driven WPB exocytosis, we performed live cell experiments. Both constructs labeled all WPBs, with the exception of immature organelles at the trans-Golgi network (Figure 4Ci). Figure 4Cii-iii compares the kinetics and extent of WPB exocytosis in control cells expressing the WPB-specific protein Proregion-EGFP[23] (black) with that in EGFP-Slp4-a–expressing cells (red). Cumulative plots of WPB fusion events (Figure 4Cii bottom) are aligned to the increase in intracellular Ca^{2+} (top in Figure 4Cii). The mean delay, maximal rate, and probability of WPB fusion (P_r), are summarized in Figure 4Ciii. In EGFP-Slp4-a–expressing cells, WPB exocytosis was initially slowed, although later the rate increased and reached control values in Proregion-EGFP cells. Surprisingly, P_r was significantly increased (Figure 4Ciii). In marked contrast, expression of EGFP-MyRIP completely blocked Ca^{2+}-driven WPB exocytosis.

Quantification of the intensity of endogenous WPB-MyRIP-IR as a function of the FI of WPB-EGFP-Slp4-a showed that overexpression of EGFP-Slp4-a reduced endogenous WPB-MyRIP-IR (Figure 4Civ black symbols). In contrast, EGFP-MyRIP overexpression had only a small effect on endogenous WPB-Slp4-a-IR (Figure 4Civ gray symbols), presumably because Slp4-a, unlike MyRIP, interacts with GTP-Rab3B, GTP-Rab3D, and GDP-Rab27A on WPBs. The data show that Slp4-a and MyRIP exert opposing effects on WPB exocytosis and VWF secretion and that Slp4-a competes with MyRIP for its WPB-specific binding partner Rab27A.

Rab27A, but not Rab3B or Rab3D, regulates VWF secretion. Having established that Slp4-a acts as a positive regulator of histamine-evoked VWF secretion and that it can interact with WPB-Rab3s, we next determined the relative contributions of Rab3B, Rab3D, and Rab27A to hormone-evoked VWF secretion. To do this, we performed KDs of each Rab individually and of Rab27A and Rab3B together (Figure 5). KDs profoundly depleted each Rab, with endogenous WPB-Rab3B- and WPB-Rab27A-IR

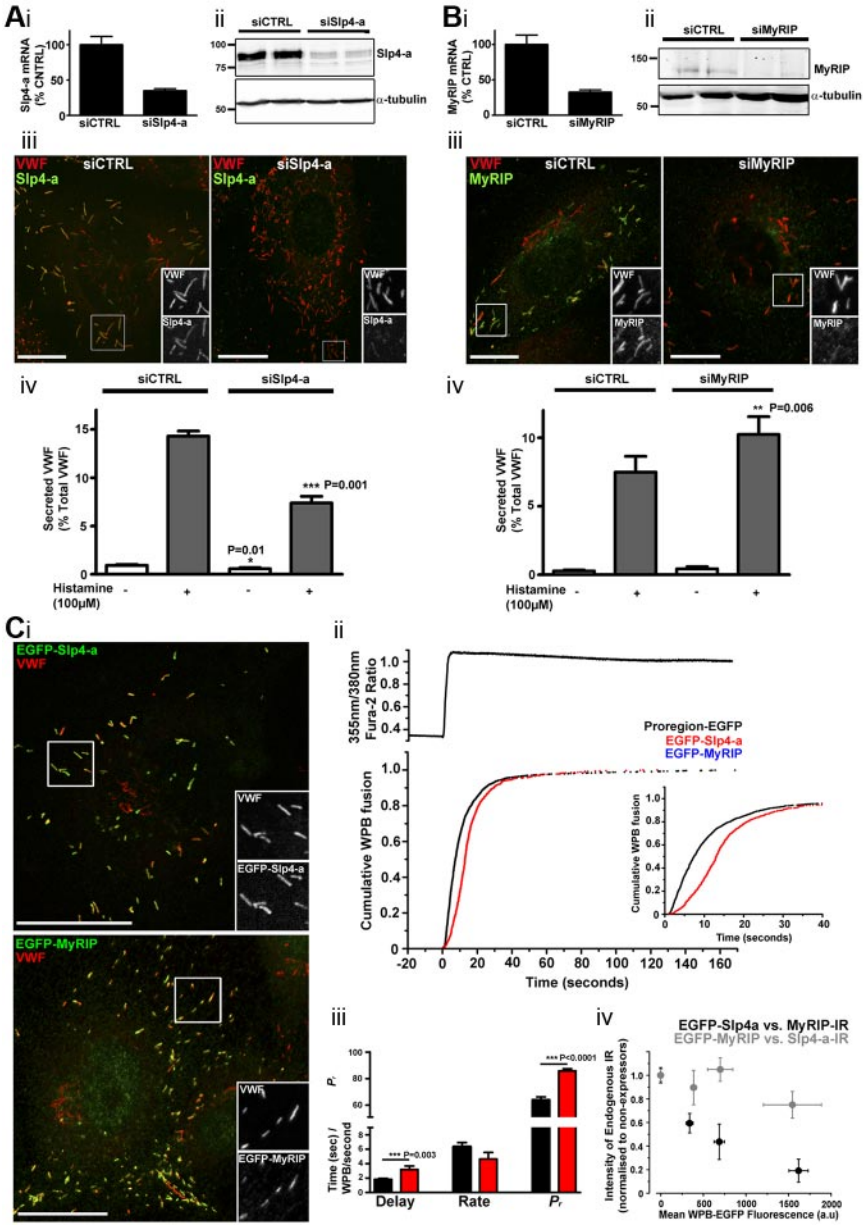

Figure 4. Slp4-a and MyRIP have opposing effects on WPB exocytosis and VWF secretion. Quantification of mRNA for Slp4-a (Ai) and MyRIP (Bi) after nucleofection with either control (siCTRL) or specific KD oligos as indicated. mRNA was depleted by 65% ± 3% (Ai) or 67% ± 3% (Bi) in KD compared with control. Data were pooled from 3 independent experiments. (Aii,Bii) Immunoblots for Slp4-a or MyRIP, respectively, after nucleofection with either control (siCTRL) or specific KD oligos as indicated. Data are representative of 3 independent experiments. Position of molecular weight markers (kDa) are shown to the left and α-tubulin used as loading control. (Aiii,Biii) Immunostaining of HUVECs for Slp4-a (rabbit Ab, green) and VWF (sheep Ab, red; Aiii) or MyRIP (goat Ab; green) and VWF (rabbit Ab, red; Biii) in control or after KD as indicated. Scale bars represent 10 μm. (Aiv,Biv) Histamine-evoked VWF secretion, quantified by ELISA, from HUVECs nucleofected with control, Slp4-a (Aiv) or MyRIP (Biv) siRNA oligos as indicated. White and gray bars represent unstimulated (vehicle alone) and histamine-stimulated conditions, respectively. Data were pooled from 3 independent experiments. A small but significant decrease in basal release was seen with Slp4-a KD (siCTRL, 0.9% ± 0.08% vs siSlp4-a, 0.57% ± 0.1% of total VWF, $P = .01$) and a trend to an increase in basal secretion for MyRIP KD (siCTRL, 0.27% ± 0.07% vs siMyRIP, 0.43% ± 0.15% of total VWF), although the latter did not reach significance ($P = .4$). (Ci) HUVECs expressing EGFP-Slp4-a (top, green) or EGFP-MyRIP (bottom, green) 24 hours after nucleofection and immunolabeled for VWF (sheep Ab; red). Grayscale images are from regions indicated by white boxes. Scale bars represent 20 μm. (Cii). Top: Fura-2 fluorescence ratio showing intracellular Ca^{2+} rise. Bottom: Cumulative plot of WPB fusion event times, normalized by their total number, in Proregion-EGFP- (black, 46 cells, 2151 fusion events), EGFP-Slp4-a– (red, 15 cells, 849 fusion events), and EGFP-MyRIP–expressing cells (blue, 21 cells, total absence of fusion events). Inset: The initial period after stimulation on an expanded time scale. (Ciii) Mean delays (seconds), maximal rates of exocytosis (WPBs/second), and probabilities of WPB exocytosis, P_r, (percent, note broken Y scale) for Proregion-EGFP (black) or EGFP-Slp4-a–expressing cells (red). (Civ) Relationship between the average intensity of endogenous WPB-Slp4-a-IR (gray) or endogenous WPB-MyRIP-IR (black) and WPB-EGFP FI (determined for individual WPBs) in cells expressing EGFP-MyRIP or EGFP-Slp4-a, respectively. In each cell (n = 32, EGFP-MyRIP; n = 30, EGFP-Slp4-a), at least 15 WPBs were quantified to determine the intensity of WPB-IR and EGFP fluorescence. WPB-IRs were scaled to the mean intensity of IR for each antigen in nonexpressing cells (n = 40) within the same experiment.

greatly diminished in both single and double KDs (Figure 5Ai-iii). KD of Rab27A also depleted WPB-MyRIP- but not WPB-Slp4-a-IR (supplemental Figure 3E). Substantial depletion of WPB-Slp4-a-IR was observed only after Rab3B/Rab27A double KD (Figure 5Aiv), and not after Rab3B or Rab27A KDs (supplemental Figures 3Eii and 5).

KD of Rab27A, but not of Rab3B or Rab3D, significantly reduced histamine-evoked VWF secretion (Figure 5Bi-ii), and no further significant decrease was seen after Rab3B/Rab27A KD. Together, the data show that Rab27A and not Rab3B or Rab3D regulate histamine-evoked VWF secretion and suggest that the influence on exocytosis of their common effector, Slp4-a, is mediated via Rab27A alone.

The probability of WPB exocytosis is unaffected by reductions in WPB-Rab27A concentration with increasing WPB pool size. The inhibition of histamine-evoked VWF secretion by Rab27A KD led us to ask whether the natural reduction in WPB-Rab27A concentration with increasing WPB pool size (Figure 1B; supplemental Figure 3) was mirrored by a decrease in P_r. The reduction in WPB-Rab27A concentration with increasing WPB pool size is summarized in Figure 6A (along with the corresponding variation in WPB-MyRIP and WPB-Slp4-a levels). As the same relationship was seen in Proregion-EGFP–expressing HUVECs (supplemental Figure 6A), we could assess directly how P_r varied with WPB pool size in live cells. Figure 6B shows P_r as a function of the mean number of fluorescent WPBs per cell in the same ranges as in Figure 6A. Cells were stimulated with low or high concentrations of histamine or a maximally effective concentration of ionomycin. In each case, P_r was independent of WPB pool size. We next addressed the cellular mechanism for the reduction in WPB-Rab27A levels with increased WPB pool size.

We hypothesized that, if total cellular Rab27A levels remain unchanged with increasing WPB numbers, then Rab27A cycling between WPBs would account for the dilution in WPB-Rab27A concentration. To test this hypothesis, we took advantage of the fact that VWF content and WPB numbers in HUVECs increase with time in culture.[32] We determined how cellular levels of the WPB-specific marker Proregion and of Rab27A change with time

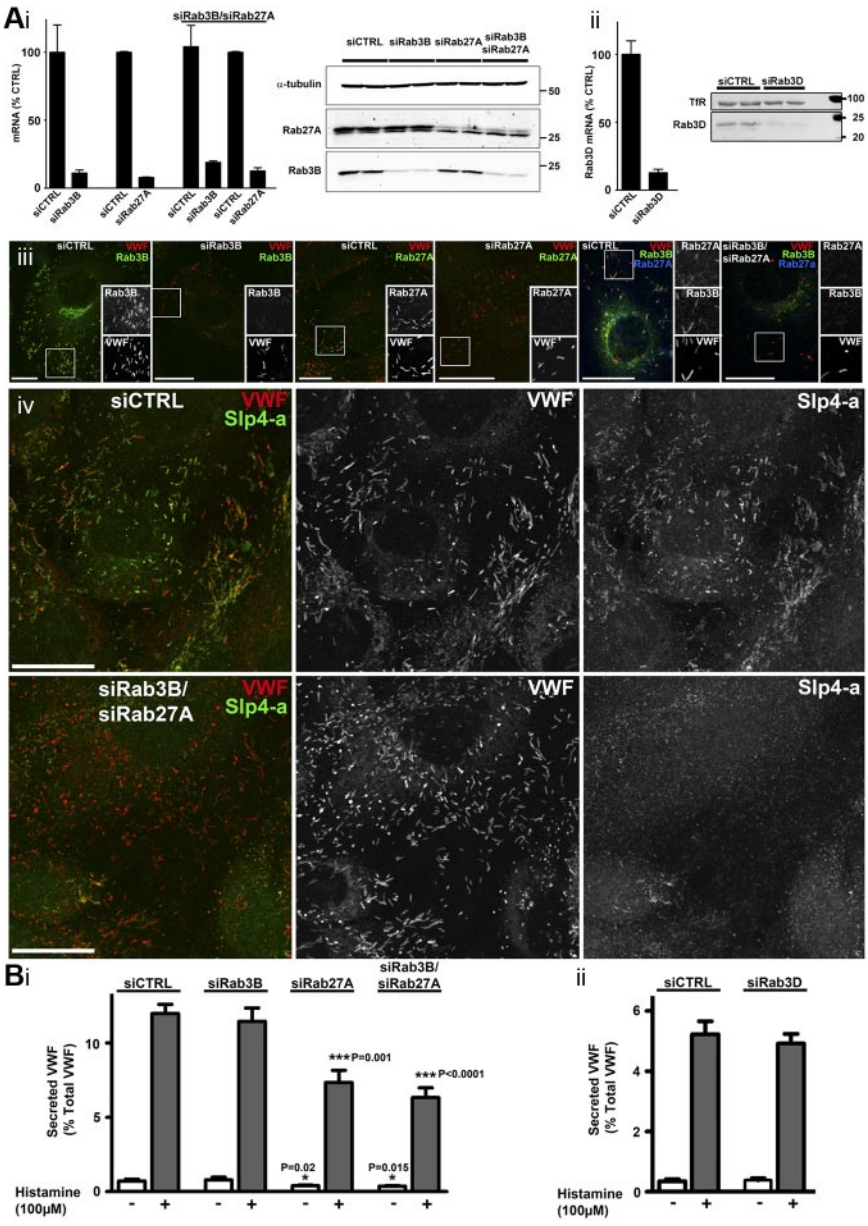

Figure 5. KD of Rab27A, but not of Rab3B or Rab3D, decreases hormone-evoked VWF secretion. (Ai-ii) Quantification of mRNA and protein after nucleofection with either control (siCTRL) or specific KD oligos as indicated. mRNA KD were Rab3B (89% ± 2%), Rab27A (92% ± 0.4%), Rab3B/Rab27A (81% ± 1%/87% ± 2%), and Rab3D (87% ± 2.6%). Data were pooled from 3-5 independent experiments. Representative immunoblots are shown. Position of molecular weight markers (kDa) are shown to the right; α-tubulin (Ai) or transferrin receptor (TfR, Aii) were used as loading controls. (Aiii) Four left panels: Immunostainings of HUVECs for endogenous Rab3B (mouse Ab, green) or Rab27A (mouse Ab, green) and VWF (sheep Ab, red) in control or KDs as indicated. Two right panels: Immunostainings of HUVECs for Rab3B (mouse Ab, green), Rab27A (rabbit Ab, blue), and VWF (sheep Ab, red). Grayscale images are from regions indicated by white boxes. Scale bars represent 20 μm. (Aiv) Immunostainings of HUVECs for Slp4-a (rabbit Ab, green in color merge on left) and VWF (sheep Ab, red in color merge on left) in control (top) or Rab3B/Rab27A KD (bottom). Scale bars represent 20 μm. (B) Histamine-evoked VWF secretion from HUVECs nucleofected with control or specific siRNA oligos for Rab3B, Rab27A, or Rab3B/Rab27A (Bi), or Rab3D (Bii) as indicated. Open bars represent control (vehicle alone); and gray bars, histamine stimulation. Data were pooled from 3 independent experiments. There was no significant difference in VWF secretion between Rab27A KD and Rab3B/Rab27A KD ($P = .26$). Compared with siCTRL, basal secretion of VWF was significantly lower in Rab27A ($P = .02$) or Rab27A/Rab3B ($P = .015$) KD experiments.

in culture. HUVEC numbers and total protein content increased with time, reaching a plateau by 96 hours (supplemental Figure 6B). As expected, levels of Proregion, adjusted for cell number, increased progressively, whereas those of Rab27A and housekeeping proteins remained unchanged (Figures 6C). Thus, HUVECs maintain a relatively constant intracellular pool of Rab27A in the face of large increases in the WPB pool size, consistent with Rab27A cycling underlying the dilution of individual WPB-Rab27A levels.

Finally, we examined how P_r changed with time after WPB formation. We performed a morphologic pulse-chase using Proregion-EGFP, and at specific times after nucleofection cells were either fixed and stained for endogenous Slp4-a or MyRIP, or used in live secretion experiments. Figure 6Di-iii shows the increase in mean number of fluorescent WPBs per cell with time after nucleofection (Figure 6Di), the mean percentage of these fluorescent WPBs that were positive for Slp4-a- (●) or MyRIP-IR (○; Figure 6Dii), and P_r (Figure 6Diii; ●). The fraction of WPBs positive for Slp4-a- or MyRIP-IR was similar at each time, consistent with the time-dependent recruitment of Rab27A.[13] At early times, when most WPBs lacked Slp4-a- or MyRIP-IR, P_r was low but increased to close to maximal levels as the fraction of WPBs positive for both effectors increased. Figure 6Diii also shows P_r values recalculated for the fraction of Slp4-a-positive WPBs at each approximate time point (○). The data suggest that P_r is closely linked to the WPB recruitment of both Slp4-a and MyRIP.

Discussion

Rab proteins on WPBs: composition and recruitment

WPBs in HUVECs and HAECs recruit Rab3B and Rab3D in addition to Rab27A. In a small number of perinuclear Rab27A-negative (immature) WPBs, we observed detectable Rab3B-IR (Figure 2C). Rabs are delivered to their target membranes by 1 of 2 routes: as newly synthesized Rabs in association with Rab

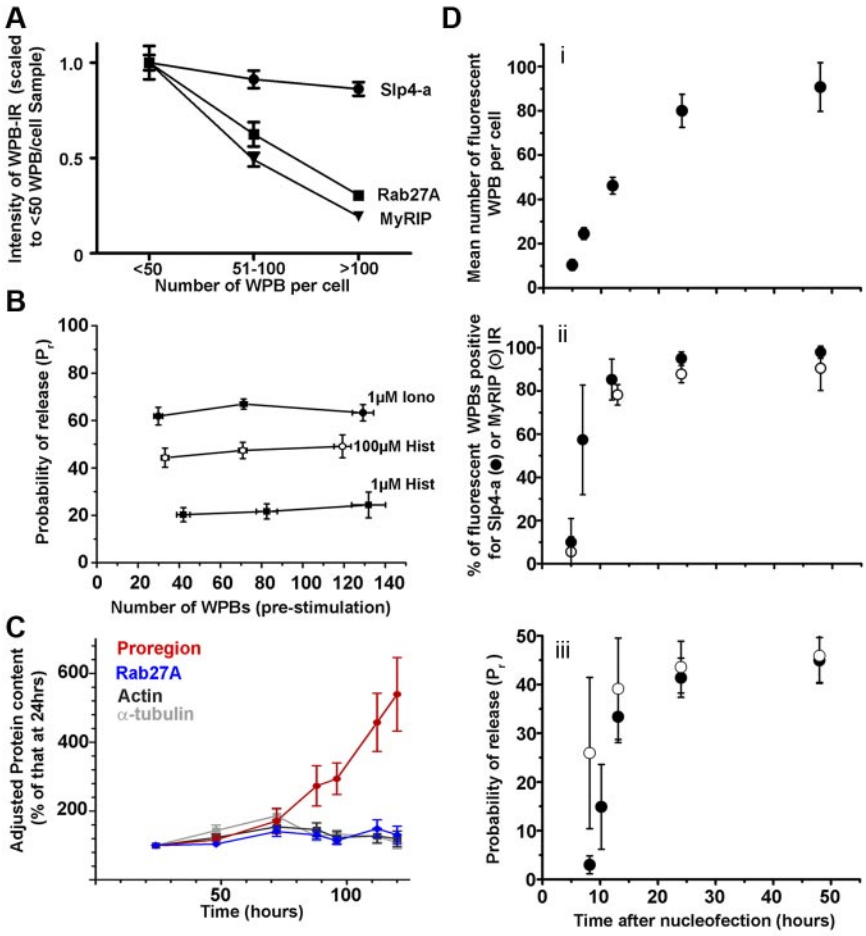

Figure 6. The probability of WPB exocytosis is maintained over a wide range of WPB-Rab27A concentrations. (A) Mean intensities of WPB-IR for endogenous Rab27A (squares), MyRIP (triangles), and Slp4-a (circles) as a function of WPB numbers per cell. Data scaled to the mean intensity for the < 50 WPBs per cell. Numbers of cells analyzed: Rab27A, 124-218; MyRIP, 17-73; Slp4-a, 16-39. For all cells with > 50 WPBs, Rab27A and MyRIP intensities of WPB-IR were significantly lower than for cells with < 50 WPBs ($P < .0001$ in all cases). For Slp4-a, corresponding WPB-Slp4-a-IR differences were not significant ($P = .14$). (B) Probabilities of WPB exocytosis, P_r, for ionomycin or histamine stimulation as indicated, plotted against the mean number of fluorescent Proregion-EGFP–containing WPBs, binned similarly to panel A. Data from 17-51 (ionomycin), 15-32 (100μM histamine), and 3-10 (1μM histamine) cells. (C) Quantification of Rab27A levels in HUVECs seeded at 1.0×10^5 cells per 3.5-cm dish and cultured in HUVEC growth medium for 24-120 hours. Growth media was replaced after 72 hours. At indicated times, the cells were counted, lysates made, and protein content determined (supplemental Figure 6B top). The intracellular content of Proregion (red), Rab27A (blue), α-tubulin (light gray), and actin (dark gray) at each time point was determined by immunoblotting, band intensities quantified in ImageJ, and corrected for cell number at corresponding time points. Cellular protein levels are presented as a percentage of those at 24 hours (data from 3 experiments, each performed in triplicate). (D) Changes in exocytosis of Proregion-EGFP–positive WPBs with time after nucleofection, same abscissa in subpanels i through iii. (Di) Increase in mean number of fluorescent WPBs per cell. (Dii) Mean percentage of Proregion-EGFP–positive WPBs displaying endogenous WPB-Slp4-a-IR (●) or WPB-MyRIP-IR (○) at the times indicated after nucleofection. (Diii) Probability of WPB exocytosis P_r for 100μM histamine stimulus (●). (○), P_r values scaled by the mean fraction of Slp4-a–positive WPBs (from Figure 6Dii, ~ 7, 12, 24, and 48 hours). Sixteen to 29 cells were analyzed at each time point.

Escort Protein (REP),[33,34] or during subsequent Rab cycling, in association with guanine-nucleotide dissociation inhibitor (GDI).[35] The key step for Rab delivery by either route is membrane insertion that requires Rab GDP-GTP exchange catalyzed by a guanine-nucleotide exchange factor (RabGEF, and possibly other as yet unidentified molecules).[36] Comparison of Rab3B τ_{recr} with Rab3B τ_{ass} or τ_{diss} (Figure 3) showed that the initial recruitment is much slower than Rab cycling on mature WPBs, suggesting that immature WPBs may preferentially recruit newly synthesized Rabs. Because newly synthesized Rab3B, Rab3D, and Rab27A share many common molecular components for delivery to target membranes,[33,34] including a RabGEF (RabGEP[36]), it is not surprising that τ_{recr} for mEGFP-Rab3B and EGFP-Rab27A to immature WPBs were similar. However, if endogenous Rab3B were more abundant than Rab27A at the protein level, as seen at the transcript level, then competition between Rab3B and Rab27A for shared molecular components could account for Rab3B-positive Rab27A-negative WPBs. Indeed, a very low GTPase activity for Rab27A may lend an additional competitive advantage to Rab3B in accessing REP.[37,38] Direct evidence for competition between secretory Rabs in HUVECs came from observations that EGFP-Rab27A or mEGFP-Rab3s' expression depleted endogenous WPB-Rab3B- or Rab27A-IR, respectively (supplemental Figure 7A-B). The primary point of competition between these Rabs is probably membrane insertion because neither cytosolic EGFP nor YFP-Rab1A, which uses distinct GEFs (and GTPase activating proteins),[39] displaced Rab3B from WPBs (supplemental Figure 7C).

Slp4-a recruitment to WPBs

We show that WPB recruitment of Slp4-a involves not only Rab27A but also Rab3B (and potentially Rab3D; Figures 3E and 5Aiv), accounting for several otherwise unexpected observations: the failure of Rab27A KD to remove Slp4-a from WPBs (supplemental Figure 3Eii), the presence of Slp4-a-IR on a population of endogenous Rab27A-negative WPBs, and retention of Slp4-a-IR on WPBs after displacement of endogenous Rab27A-IR (and MyRIP-IR) by overexpressed EGFP-Rab3s (eg, supplemental Figure 7D).

Photobleaching studies showed fast Rab3s cycling on individual WPBs, consistent with previous bulk granule bleaching studies in PC12 cells.[40] Because Slp4-a binds to Rab3s only in the GTP form (supplemental Figure 4A),[15,41] the fast τ_{ass} of EGFP-Slp4-a with mRFP-Rab3–expressing WPBs (Figure 3E) indicates that Slp4-a cycling is strongly influenced by the underlying cycling of Rab3s. Rab27A also cycled, but its τ_{ass} was very slow, consistent with studies in PC12 cells.[40] Slow Rab27A cycling could reflect the fast constitutive GDP-GTP exchange and slow GTP hydrolysis rates reported to hold Rab27A predominantly as GTP-Rab27A on SGs.[37] Unlike for Rab3s, conversion to GDP-Rab27A is not associated with loss from membranes.[37] Whether this arises because Rab27A is a poor substrate for GDI or because access to GDI is hindered by binding to effectors in the GDP-state (eg, Slp4-a, coronin-3)[41,42] remains to be established. The cycling of EGFP-Slp4-a on mRFP-Rab27A–expressing WPBs mirrored the very slow cycling of Rab27A itself, presumably because Slp4-a,

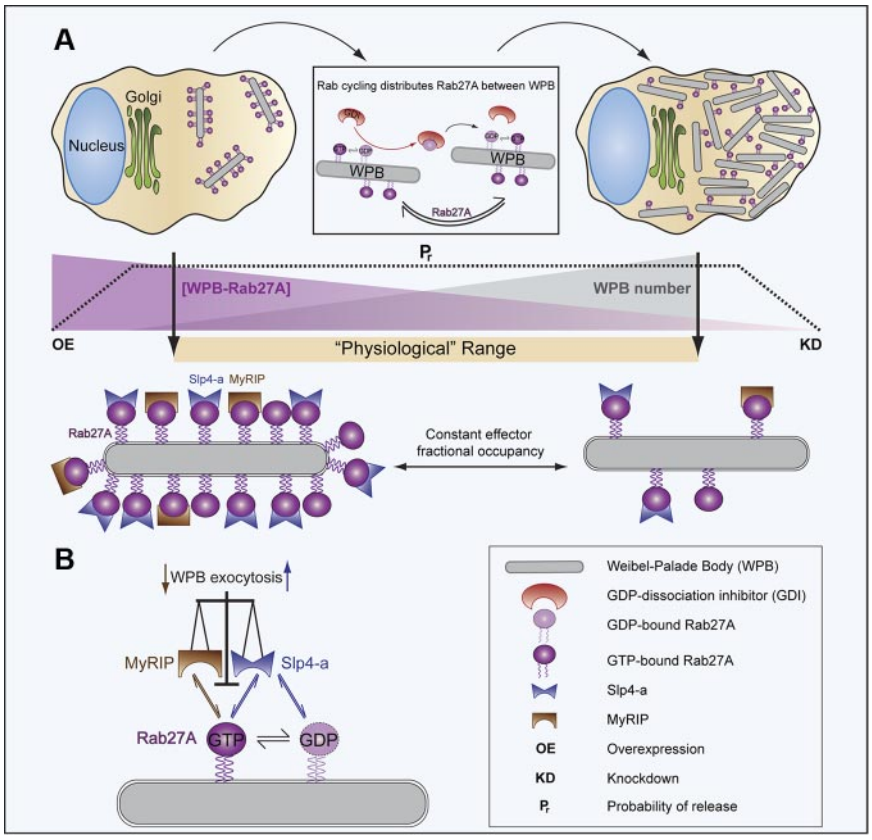

Figure 7. Slp4-a and MyRIP acting via Rab27A control the probability of WPB exocytosis independently of WPB pool size. (A) Rab27A cycles between the cytosol and the WPB membrane, a process thought to be dependent on GDP-dissociation inhibitor (GDI; rectangular insert, cellular components are not drawn to scale). Rab cycling distributes Rab27A approximately evenly between all WPBs within the cell. Because the cellular content of Rab27A remains constant in culture, increases in WPB pool size (gray gradient) over a "Physiologic range" (beige bar) result in a decrease in the amount of Rab27A on individual WPBs (purple gradient). The probability of WPB release (P_r, dashed line) remains constant over this "Physiologic range" of WPB pool sizes, indicating that the control of WPB exocytosis cannot solely depend on the absolute amount of WPB-Rab27A. As long as the cellular content of Rab27A (and its effectors) remains constant, the steady-state fractional occupancy of Rab27A by its effectors will also be constant, irrespective of the absolute Rab27A concentration on individual WPBs. This raises the possibility that the fractional occupancy of Rab27A by its effectors, rather than just the absolute amount of these molecules, sets the P_r. Substantial depletion (by KD, extreme right of panel A) or high overexpression (OE, extreme left in panel A; data not shown) of Rab27A results in a reduction in P_r. (B) WPB exocytosis is determined by the balance of occupancy of WPB-Rab27A by negative (MyRIP that binds only GTP-Rab27A) and positive (Slp4-a that binds both GTP- and GDP-Rab27A) effectors. Manipulations that alter either effector concentration or cellular Rab27A levels can perturb the fractional occupancy of WPB-Rab27A by its effectors, resulting in changes (small vertical arrows) in the probability of WPB exocytosis.

unlike other Rabs, binds to both GTP and GDP-bound states of Rab27A.[41] The fact that EGFP-Slp4-a alone cycled as fast as in the presence of exogenous Rab3B or Rab3D indicates that Slp4-a associates with endogenous WPB-Rab3s in living HUVECs.

Slp4-a and MyRIP have opposite effects on WPB exocytosis

Our data show that Slp4-a acts as a positive regulator of hormone-evoked WPB exocytosis and confirm that MyRIP is a negative regulator of this process.[14] The latter is also consistent with MyRIP's reported role in phorbol 12-myristate 13-acetate (PMA)–stimulated secretion of VWF.[13] The results for Slp4-a are particularly interesting because this molecule is reported to be inhibitory for SG exocytosis in other secretory cells.[20,43] This inhibitory effect is thought to arise through an increased tendency to form nonproductive docked complexes with PM syntaxins, although the underlying kinetics of exocytosis remain unchanged. In contrast, we found that Slp4-a expression increased P_r in response to ionomycin and slowed the initial phase of WPB fusion. The latter could involve the aforementioned processes,[20,43] but this remains to be established.

A striking consequence of EGFP-Slp4-a overexpression was a reduction in the intensity of endogenous WPB-MyRIP-IR, showing that these effectors compete for their common binding partner, Rab27A. This raises the intriguing possibility that the increase in P_r observed on EGFP-Slp4-a expression might arise simply from the competitive displacement of endogeous MyRIP from GTP-Rab27A on WPBs. Indeed, the relatively modest effect of EGFP-Slp4-a expression (20%-25% increase in WPB exocytosis), was reminiscent of the effect of MyRIP KD (~ 15%-25% increase in VWF secretion). Conversely, EGFP-MyRIP expression should displace endogenous Slp4-a from GTP-Rab27A bound to WPBs, shifting the occupancy of GTP-Rab27A toward MyRIP and thus inhibiting WPB exocytosis. Indeed, we observed a complete inhibition of WPB exocytosis, although depletion of endogenous Slp4-a-IR from WPBs was masked by the capacity of WPB-Rab3s to recruit Slp4-a to WPBs. Compared with the relatively small effect of MyRIP depletion from WPBs, it indicates that endogenous WPB-MyRIP levels exert a relatively weak brake on WPB exocytosis.

Rab27A regulates VWF secretion

Rab27A KD caused a significant inhibition of both unstimulated and stimulated VWF secretion, whereas Rab3B or Rab3D depletion had no effect (Figure 5B). A reduction in unstimulated secretion in other KD conditions (eg, Slp4-a) also mirrored the effect on stimulated secretion. Because the majority of unstimulated VWF secretion arises from basal release of WPBs,[44] this indicates that the same molecular machinery influences stimulated and basal VWF secretion. Our Rab27A KD data differ from a previous study reporting a substantial increase in PMA-stimulated VWF secretion,[13] presumably reflecting differences in the mechanisms by which PMA and hormone trigger VWF secretion. An increase in histamine-evoked VWF secretion was also reported in that study[13]; however, those results were equivocal because of a 3-fold increase in unstimulated VWF release caused by Rab27A KD.

Overexpression of epitope-tagged Rab3D has also been reported to inhibit hormone-evoked VWF secretion,[3] and we observed the same result (supplemental Figure 7E). However, we found that Rab3D overexpression was accompanied by loss of endogenous WPB-Rab27A-IR and MyRIP-IR (supplemental Figure 7Bii), although WPB-Slp4-a-IR was still observed, consistent with Slp4-a binding to WPB-Rab3s (supplemental Figure 7D). The data suggest that the effect of Rab3D overexpression arises through

competitive displacement of Rab27A from WPBs and that, despite recruiting Slp4-a to WPBs, Rab3s do not support the positive action of Slp4-a on VWF secretion. The latter idea is consistent with previous data in PC12 cells.[21] Slp4-a binds to GTP- and GDP-Rab27A states,[41] whereas MyRIP binds to GTP-Rab27A only.[45] If Slp4-a and MyRIP compete for WPB-Rab27A, as suggested by data in Figure 4Civ, then the capacity of Slp4-a to bind GDP-Rab27A could confer a competitive advantage over MyRIP in a positive drive toward exocytosis.

KD of Rab3B (and Rab3D) suggests little or no role for these Rabs in controlling WPB exocytosis, raising the intriguing question as to their function on the WPBs. Rab3B and Rab3D are implicated in processes not directly related to control of exocytosis, including the regulation of catecholamine uptake into SGs,[46] receptor transcytosis,[47] SG-microtubule interactions,[48] and SG maturation.[49] The function of Rab3s on WPBs remains to be established.

The probability of WPB exocytosis does not depend solely on the absolute WPB-Rab27A concentration over the endogenous range

Despite marked intercellular variations in the amount of endogenous Rab27A (and MyRIP) on WPBs because of increasing WPB pool size (Figures 1B and 6A; supplemental Figure 3A-B), P_r was constant for a given stimulus strength (Figure 6B). This suggests that P_r is not determined solely by the absolute amount of Rab27A and its effectors on WPBs, although some finite amount of each must be required. Instead, some other parameter(s) must be important in determining P_r. We found that the total cellular content of Rab27A remains essentially constant with time in culture, and our preliminary results indicate that the same is true for MyRIP and Slp4-a (and Rab3B). In this case, the steady-state fractional occupancy of Rab27A by its effectors should also remain constant, irrespective of the absolute amounts of Rab27A on any individual organelle. This raises the possibility that the fractions of WPB-Rab27A molecules occupied by MyRIP and Slp4-a are the crucial factor in determining P_r. Most newly formed WPBs lack endogenous Slp4-a-IR, MyRIP-IR (Figure 6Dii), Rab27A-IR[12] (and Rab3B-IR, Figure 2B), and for these organelles P_r was very low (Figure 6Diii). The close correlation between the increase in P_r (Figure 6Diii) and increase in the fraction of WPBs with detectable Slp4-a- and MyRIP-IR (Figure 6Dii) shows that the capacity to undergo exocytosis is closely linked to acquisition of both effector molecules. By assuming that WPBs completely lacking these components are not fusion-competent, we found that newly formed WPBs (7 hours after nucleofection) with detectable Slp4-a-IR and MyRIP-IR had a P_r not much lower than that seen for much older organelles (Figure 6Diii, ○). The slightly higher P_r seen for older WPBs may reflect their predominantly peripheral localization and closer apposition to the PM. Manipulations that alter the steady-state fractional occupancy of Rab27A (eg, overexpression or KD of Slp4-a or MyRIP) change P_r and VWF secretion. Substantial reductions in WPB-Rab27A levels after Rab27A KD simulate a return toward the "immature state" where Rab27A, MyRIP, and Slp4-a are missing, rendering WPBs less responsive to stimulation.

In conclusion, WPBs recruit multiple Rabs; however, our data suggest that Slp4-a and MyRIP acting via Rab27A regulate WPB exocytosis and VWF secretion. Our data indicate that the fractional occupancy of WPB-Rab27A by its effectors rather than just the absolute amount of these molecules on WPBs is an important factor in determining P_r. Thus, by simply maintaining the cellular content of Rab27A and its effectors at approximately constant levels, ECs maintain P_r constant irrespective of WPB pool size (Figure 7). This provides a simple mechanism to ensure a coordinated and proportionate response of the EC population to external stimuli of varying intensity.

Acknowledgments

M.J.H. and T.C. were supported by the United Kingdom Medical Research Council (reference codes U117570589 and U117573808).

Authorship

Contribution: R.B., N.H., N.K., L.K., B.P., A.M., A.-V.F., and T.C. performed research and analyzed data; A.M. and M.R. contributed vital reagents; and R.B., N.H., N.K., A.-V.F., M.J.H., and T.C. designed the research and wrote the paper.

Conflict-of-interest disclosure: The authors declare no competing financial interests.

The current affiliation for M.J.H. is Microbiology Services Colindale, Health Protection Agency, London, United Kingdom.

Correspondence: Tom Carter, Department of Physical Biochemistry, National Institute for Medical Research, The Ridgeway, Mill Hill, London NW7 1AA, United Kingdom; e-mail: tcarter@nimr.mrc.ac.uk.

References

1. Rondaij MG, Bierings R, Kragt A, van Mourik JA, Voorberg J. Dynamics and plasticity of Weibel-Palade bodies in endothelial cells. *Arterioscler Thromb Vasc Biol.* 2006;26(5):1002-1007.
2. Fu J, Naren AP, Gao X, Ahmmed GU, Malik AB. Protease-activated receptor-1 activation of endothelial cells induces protein kinase Calpha-dependent phosphorylation of syntaxin 4 and Munc18c: role in signaling p-selectin expression. *J Biol Chem.* 2005;280(5):3178-3184.
3. Knop M, Aareskjold E, Bode G, Gerke V. Rab3D and annexin A2 play a role in regulated secretion of vWF, but not tPA, from endothelial cells. *EMBO J.* 2004;23(15):2982-2992.
4. Konig J, Prenen J, Nilius B, Gerke V. The annexin II-p11 complex is involved in regulated exocytosis in bovine pulmonary artery endothelial cells. *J Biol Chem.* 1998;273(31):19679-19684.
5. Matsushita K, Morrell CN, Cambien B, et al. Nitric oxide regulates exocytosis by S-nitrosylation of N-ethylmaleimide-sensitive factor. *Cell.* 2003;115(2):139-150.
6. Pulido IR, Jahn R, Gerke V. VAMP3 is associated with endothelial Weibel-Palade bodies and participates in their Ca(2+)-dependent exocytosis. *Biochim Biophys Acta.* 2011;1813(5):1038-1044.
7. Disse J, Vitale N, Bader MF, Gerke V. Phospholipase D1 is specifically required for regulated secretion of von Willebrand factor from endothelial cells. *Blood.* 2009;113(4):973-980.
8. Fukuda M. Regulation of secretory vesicle traffic by Rab small GTPases. *Cell Mol Life Sci.* 2008;65(18):2801-2813.
9. Silva AP, Kaufmann JE, Vivancos C, et al. Neuropeptide Y expression, localization and cellular transducing effects in HUVECs. *Biol Cell.* 2005;97(6):457-467.
10. Mori R, Ikematsu K, Kitaguchi T, et al. Release of TNF-alpha from macrophages is mediated by small GTPase Rab37. *Eur J Immunol.* 2011;41:3230-3239.
11. Karniguian A, Zahraoui A, Tavitian A. Identification of small GTP-binding rab proteins in human platelets: thrombin-induced phosphorylation of rab3B, rab6, and rab8 proteins. *Proc Natl Acad Sci U S A.* 1993;90(16):7647-7651.
12. Hannah MJ, Hume AN, Arribas M, et al. Weibel-Palade bodies recruit Rab27 by a content-driven, maturation-dependent mechanism that is independent of cell type. *J Cell Sci.* 2003;116(19):3939-3948.
13. Nightingale TD, Pattni K, Hume AN, Seabra MC, Cutler DF. Rab27a and MyRIP regulate the amount and multimeric state of VWF released from endothelial cells. *Blood.* 2009;113(20):5010-5018.
14. Rojo Pulido I, Nightingale TD, Darchen F, Seabra MC, Cutler DF, Gerke V. Myosin Va acts in concert with Rab27a and MyRIP to regulate acute von-Willebrand factor release from endothelial cells. *Traffic.* 2011;12(10):1371-1382.
15. Coppola T, Frantz C, Perret-Menoud V,

Gattesco S, Hirling H, Regazzi R. Pancreatic beta-cell protein granuphilin binds Rab3 and Munc-18 and controls exocytosis. *Mol Biol Cell.* 2002;13(6):1906-1915.

16. Fukuda M, Imai A, Nashida T, Shimomura H. Slp4-a/granuphilin-a interacts with syntaxin-2/3 in a Munc18–2-dependent manner. *J Biol Chem.* 2005;280(47):39175-39184.
17. Gomi H, Mizutani S, Kasai K, Itohara S, Izumi T. Granuphilin molecularly docks insulin granules to the fusion machinery. *J Cell Biol.* 2005;171(1):99-109.
18. Tomas A, Meda P, Regazzi R, Pessin JE, Halban PA. Munc 18-1 and granuphilin collaborate during insulin granule exocytosis. *Traffic.* 2008;9(5):813-832.
19. Torii S, Zhao S, Yi Z, Takeuchi T, Izumi T. Granuphilin modulates the exocytosis of secretory granules through interaction with syntaxin 1a. *Mol Cell Biol.* 2002;22(15):5518-5526.
20. Wang H, Ishizaki R, Kobayashi E, Fujiwara T, Akagawa K, Izumi T. Loss of granuphilin and loss of syntaxin-1A cause differential effects on insulin granule docking and fusion. *J Biol Chem.* 2011; 286(37):32244-32250.
21. Fukuda M, Kanno E, Saegusa C, Ogata Y, Kuroda TS. Slp4-a/granuphilin-a regulates dense-core vesicle exocytosis in PC12 cells. *J Biol Chem.* 2002;277(42):39673-39678.
22. Brozzi F, Diraison F, Lajus S, et al. Molecular mechanism of myosin Va recruitment to dense core secretory granules. *Traffic.* 2011;13(1):54-69.
23. Erent M, Meli A, Moisoi N, et al. Rate, extent and concentration-dependence of histamine-evoked Weibel-Palade body exocytosis determined from individual fusion events in human endothelial cells. *J Physiol.* 2007;583:195-212.
24. McDouall RM, Batten P, McCormack A, Yacoub MH, Rose ML. MHC class II expression on human heart microvascular endothelial cells: exquisite sensitivity to interferon-gamma and natural killer cells. *Transplantation.* 1997;64(8): 1175-1180.
25. Knipe L, Meli A, Hewlett L, et al. A revised model for the secretion of tPA and cytokines from cultured endothelial cells. *Blood.* 2010;116(12): 2183-2191.
26. Livak KJ, Schmittgen TD. Analysis of relative gene expression data using real-time quantitative PCR and the 2(-Delta Delta C(T)) method. *Methods.* 2001;25(4):402-408.
27. Kiskin NI, Hellen N, Babich V, et al. Protein mobilities and P-selectin storage in Weibel-Palade bodies. *J Cell Sci.* 2010;123(17):2964-2975.
28. Dundr M, Hoffmann-Rohrer U, Hu Q, et al. A kinetic framework for a mammalian RNA polymerase in vivo. *Science.* 2002;298(5598):1623-1626.
29. Michaux G, Dyer CE, Nightingale TD, Gallaud E, Nurrish S, Cutler DF. A role for Rab10 in von Willebrand factor release discovered by an AP-1 interactor screen in C. elegans. *J Thromb Haemost.* 2011;9(2):392-401.
30. Grosshans BL, Ortiz D, Novick P. Rabs and their effectors: achieving specificity in membrane traffic. *Proc Natl Acad Sci U S A.* 2006;103(32): 11821-11827.
31. Bulinski JC, Odde DJ, Howell BJ, Salmon TD, Waterman-Storer CM. Rapid dynamics of the microtubule binding of ensconsin in vivo. *J Cell Sci.* 2001;114(21):3885-3897.
32. Howell GJ, Herbert SP, Smith JM, et al. Endothelial cell confluence regulates Weibel-Palade body formation. *Mol Membr Biol.* 2004;21(6):413-421.
33. Cremers FP, Armstrong SA, Seabra MC, Brown MS, Goldstein JL. REP-2, a Rab escort protein encoded by the choroideremia-like gene. *J Biol Chem.* 1994;269(3):2111-2117.
34. Figueiredo AC, Wasmeier C, Tarafder AK, Ramalho JS, Baron RA, Seabra MC. Rab3GEP is the non-redundant guanine nucleotide exchange factor for Rab27a in melanocytes. *J Biol Chem.* 2008;283(34):23209-23216.
35. Pfeffer SR, Dirac-Svejstrup AB, Soldati T. Rab GDP dissociation inhibitor: putting rab GTPases in the right place. *J Biol Chem.* 1995;270(29): 17057-17059.
36. Tarafder AK, Wasmeier C, Figueiredo AC, et al. Rab27a targeting to melanosomes requires nucleotide exchange but not effector binding. *Traffic.* 2011;12(8):1056-1066.
37. Kondo H, Shirakawa R, Higashi T, et al. Constitutive GDP/GTP exchange and secretion-dependent GTP hydrolysis activity for Rab27 in platelets. *J Biol Chem.* 2006;281(39):28657-28665.
38. Larijani B, Hume AN, Tarafder AK, Seabra MC. Multiple factors contribute to inefficient prenylation of Rab27a in Rab prenylation diseases. *J Biol Chem.* 2003;278(47):46798-46804.
39. Fukuda M. TBC proteins: GAPs for mammalian small GTPase Rab? *Biosci Rep.* 2011;31(3):159-168.
40. Handley MT, Haynes LP, Burgoyne RD. Differential dynamics of Rab3A and Rab27A on secretory granules. *J Cell Sci.* 2007;120(6):973-984.
41. Fukuda M. Slp4-a/granuphilin-a inhibits dense-core vesicle exocytosis through interaction with the GDP-bound form of Rab27A in PC12 cells. *J Biol Chem.* 2003;278(17):15390-15396.
42. Kimura T, Kaneko Y, Yamada S, et al. The GDP-dependent Rab27a effector coronin 3 controls endocytosis of secretory membrane in insulin-secreting cell lines. *J Cell Sci.* 2008;121(18): 3092-3098.
43. Tsuboi T, Kitaguchi T, Karasawa S, Fukuda M, Miyawaki A. Age-dependent preferential dense-core vesicle exocytosis in neuroendocrine cells revealed by newly developed monomeric fluorescent timer protein. *Mol Biol Cell.* 2010;21(1):87-94.
44. Giblin JP, Hewlett LJ, Hannah MJ. Basal secretion of von Willebrand factor from human endothelial cells. *Blood.* 2008;112(4):957-964.
45. El-Amraoui A, Schonn JS, Kussel-Andermann P, et al. MyRIP, a novel Rab effector, enables myosin VIIa recruitment to retinal melanosomes. *EMBO Rep.* 2002;3(5):463-470.
46. Francis SC, Sunshine C, Kirk KL. Coordinate regulation of catecholamine uptake by rab3 and phosphoinositide 3-kinase. *J Biol Chem.* 2002; 277(10):7816-7823.
47. Van IJzendoorn SC, Tuvim MJ, Weimbs T, Dickey BF, Mostov KE. Direct interaction between Rab3b and the polymeric immunoglobulin receptor controls ligand-stimulated transcytosis in epithelial cells. *Dev Cell.* 2002;2(2):219-228.
48. Hanania R, Sun HS, Xu K, Pustylnik S, Jeganathan S, Harrison RE. Classically activated macrophages use stable microtubules for matrix metalloproteinase-9 (MMP-9) secretion. *J Biol Chem.* 2012;287(11):8468-8483.
49. Kogel T, Gerdes HH. Roles of myosin Va and Rab3D in membrane remodeling of immature secretory granules. *Cell Mol Neurobiol.* 2010;30(8): 1303-1308.